Electrophysical Properties of Polymer Electrolyte Membranes: A Random Network Model

M. Eikerling, A. A. Kornyshev,*,† and U. Stimming‡

Institut für Energieverfahrenstechnik, Forschungszentrum "Jülich" GmbH, D-52425 Jülich, Germany

Received: July 14, 1997; In Final Form: October 2, 1997[⊗]

A random network model of charge transport in porous polymer membranes is proposed and investigated by means of an effective medium theory. Specific conductivity and geometrical capacity (dielectric constant) of membranes are calculated in dependence of water content, taking swelling effects into account. The conductivity shows a quasi-percolation type dependence, growing above a certain critical water content, while taking below it a value typical of residual conductivity in dry membranes. The geometrical capacity can show an increase with water content or it can undergo a maximum at the percolation threshold, depending on the model parameters. The theoretical findings are in line with experimental observations of the membrane complex impedance as a function of water content. The results suggest a frame for classification of different types of polymer membranes with regard to their performance, depending on swelling properties.

I. Introduction

A. Ion Exchange Membranes. Low-temperature proton exchange membrane fuel cells (PEMFC) are seen today as the most promising energy suppliers for vehicles.[1] The role of electrolyte in PEMFC is played by a proton exchange membrane (PEM). Proton-conducting materials are, therefore, of great current interest for modern energy process engineering. Demands on PEMs are high proton conductivity, good insulation of electronic currents, good separation of fuel (H_2 or methanol) and oxygen (air), chemical and thermal stability of the material, and *low cost*.

The optimization of PEMs, meeting these high demands, is a key task in making PEMFC-powered systems competitive with combustion engines. This motivates efforts toward a better understanding on "microscopic" and "statistical" levels of how the membrane operates.

The microporous PEMs are conductive only when they are soaked with water. In their working state they can be swollen to a degree of about 20−30% by weight.[2] Preventing the membranes from "drying out" under working conditions, i.e., the water management, is one of the most endeavoring tasks in low-temperature fuel cell research. Indeed, the electroosmosis in the course of the current passage across the membrane, as well as the production of new portions of water at the cathode, gives rise to a fluctuating inhomogeneous distribution of water in the membrane. A robust membrane, the mean conductance of which is less sensitive to drying, would survive such fluctuations, while a feeble one would either deteriorate, or show unstable performance.

Generally, the transport of different species, including fuel, oxygen, and reaction products, has to be considered during operation of the PEMFC. As a start one may, however, consider only the proton transport and study the membrane ex situ, i.e., out of the fuel cell configuration. In this case we do not have to deal with a complicated picture of reactions in porous electrodes on both sides of the membrane, and the reactants and products transport to and from the reaction zone. The goal of such a study would be to simulate the complex impedance of the bare membrane, the first measurements of which have been already reported.[3] Comparison of the model predictions and the experiments may then help to distinguish mechanisms of proton transport depending on membrane porous structure, water permeation, etc. This is the subject of the present article.

We shall focus on *perfluorinated sulfonic acid membranes*, i.e., the famous NAFION and its derivatives, which are most widely studied experimentally. If not the most promising among polymer membranes, they provide at least the most reproducible performance in PEMFC, having a good mechanical stability and high proton conductivity.

B. Chemical Structure of the Polymer, the Inverted Micelle Model of PEM, and Proton Conduction Mechanisms. The polymer molecule of the perfluorinated sulfonic acid consists of a hydrophobic polytetrafluoroethylen (PTFE) backbone which terminates by a hydrophilic polar headgroup SO_3H.[4,5] These constituents are responsible for the morphological structure of the membranes: The emerging structure in the hydrated state possesses hydrophilic ionic clusters which contain the solvated SO_3^--heads, water, and counterions (predominantly H^+ but depending on pretreatment also some Na^+, K^+ with coions). These cluster regions are connected by short and narrow channels. The water-containing cluster network is "embedded" in the surrounding, sponge-like medium of the hydrophobic PTFE-backbones, which provides the morphological stability of the membranes. X-ray investigations by Starkweather[6] are interpreted in favor of a lamellar, hexagonal structure of the fluorocarbon chains. Two rows of fluorocarbon chains build walls of about 1 nm thickness. The separation of the polymer constituents in hydrophobic regions and the water-filled hydrophilic clusters is a consequence of the tendency to make the interface between the water of hydration and the hydrophobic polymer backbones as small as possible. The described ion-cluster morphology is suggested on the basis of a number of experimental studies which employ different techniques, including X-ray studies, NMR, IR, electron microscopy, etc.[7]

An important characteristic of the membranes is their equivalent weight,

$$\mathrm{EW} = \frac{\text{g dry polymer}}{\text{moles of ion exchange places } (SO_3^-)}$$

* Corresponding author. E-mail: A. Kornyshev@fz-juelich.de.

† Also a staff member of the A. N. Frumkin Institute of Electrochemistry of the Russian Academy of Sciences, 117071 Moscow, Russia.

‡ Present address: Physik-Department E19, Fakultät für Physik, Technische Universität München, Institut für Festkörperphysik und Technische Physik, James Franck Strasse 1, D-85747 Garching, Germany.

⊗ Abstract published in *Advance ACS Abstracts,* November 15, 1997.

S1089-5647(97)02288-8 CCC: $14.00 © 1997 American Chemical Society

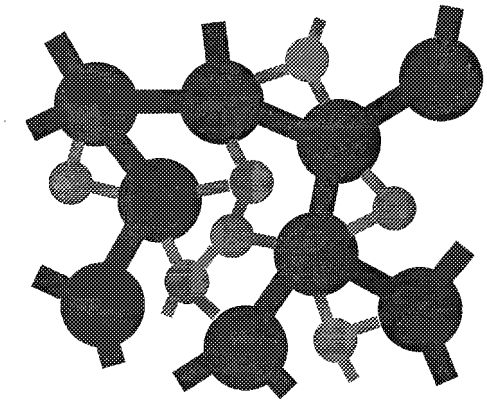

(a)

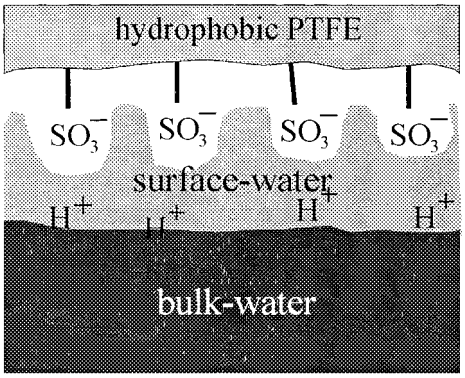

(b)

Figure 1. Inverted micellar structure model of PEM with ionic clustering. Two types of pores are distinguished. Water-filled, swollen pores, referred to in the text as blue pores, are depicted here as large, black circles. Dry pores, called red pores in the text, are shown as small, gray circles. In panel b the conditions at the surfaces of blue and red cavities (pores and channels) with localized SO_3^--groups and positive charges moving along the surface water layer are depicted.

The higher the EW, the lower the conductivity and the higher the morphological stability.

A widely known model of PEM is due to Gierke[8] who proposed an inverted micellar structure in which the ionic clusters exist as interconnected, spherical domains (*pores*), Figure 1. An average pore in the swollen state has a diameter of 4−5 nm, contains ∼70 fixed SO_3^--groups sitting at the inner pore surface with a spacing ∼1 nm, and is filled with ∼1000 water molecules. The effective radius of an ion exchange site (SO_3^-) is ∼0.25 nm. The channels connecting the pores have diameter and length ∼1 nm. According to Gierke[8] pores exist even in the dry state with diameter ∼1.8 nm and ∼26 SO_3^--groups per pore. Although the inverted micellar structure model seems convincing from an experimental point of view, one should be aware that there were also other models suggested and that no single view on the structure of these polymer membranes has been established yet.[4,9] The model of Gierke, however, has certain advantages for the simulation of conductance we are aiming at since it is most easily mapped on a "random network"-type model.[10]

The idea of inverted micelles taking up the water in these membranes has found broad acceptance, and this is an active field of experimental research,[11] whereas the existence of channels has never been verified. Note, however, that the mapping of membrane structure on a random network would result in a phenomenological description, which is not literallybased on the Gierke model, though it implies the concept of pores and channels. The "shape" of the elements forming the network appears in the model only through geometrical factors, which relate specific conductivities with elemental conductances. The distinction between pores and channels is not essential as far as we will not ascribe different values of conductances to them (cf. section IV.A).

There is only weak cross-linking of the polymer chains. The microporous NAFION-type membranes are thermoplastic. The swelling upon water uptake is controlled by a balance between internal osmotic pressure of the pores, formed by repulsive hydration and attractive van der Waals forces, and the elastic forces exerted by the polymer matrix. The cluster growth is a combination of cluster expansion and a continuous redistribution of exchange sites. There are fewer clusters in a fully hydrated sample.[8]

Two different water environments in the membrane can be distinguished. A certain amount of water is needed for the solvation of the SO_3^--groups. This water is tightly bound close to the inner-pore surfaces. Due to the effect of the hydrophobic PTFE-backbones, there are less hydrogen bonds per water molecule near the pore surfaces than in bulk water and the remaining bonds are stiffer.[12,13] The uptake of additional water fills the volumes of pores and behaves more bulklike.

Proton transport is frequently discussed in terms of two different mechanisms:[13] the *Grotthus mechanism* (orientational modes assisted proton hopping, also called *structural diffusion*) and the so-called *vehicle mechanism*. The latter implies the diffusion of protons on a vehicle, as H_3O^+-ion or larger complexes, with a simultaneous counterdiffusion of water molecules. This mechanism is favored by disorder (weaker hydrogen bonding); it is hardly realized in a dry membrane with a residual water inside, but it could be activated upon filling of pores with additional portions of water. There are problems in discriminating between the two mechanisms, and it is possible that to a certain extent, dependent on the water content, both of them contribute to the charge transport across the membrane.[14]

C. What Are the Phenomena? In this paper we will focus on the conductivity and related properties as functions of the water content. Our purpose will be to find out which of the membrane parameters may favor better performance for a given water content. Two notions are frequently used as the definitions of the water content:

$$\lambda = \frac{\text{number of water molecules}}{\text{number of ionic headgroups}}$$

or

$$W = \frac{\text{g water}}{\text{100 g of dry polymer}}$$

λ and W are related by a simple proportionality.[2] In this paper we shall use the notation w which characterizes the extra water content of the membrane (≡ percentage gain in weight by weight of water). The "dry" membrane with $w = 0$ still contains the water molecules at the surface. This residual water content amounts to $\lambda \approx 5-6$. It can only be removed under vacuum conditions at high temperatures, which partly destroy the membrane structure. For the fuel cell performance only the range $w > 0$ is relevant. Swelling of the membranes is possible up to $w \sim 20-30$.

The functional dependence of the conductivity on w is determined by the type of membrane and its EW, pretreatment of the membrane (e.g., boiling in acidic solutions or in destilled water, etc.), temperature, as well as other external variables, and the mechanism of water uptake. Numerous studies on these dependencies can be found in the literature.[4,16] Note that water uptake from liquid water, i.e., *impregnation*, is roughly twice as high as the uptake from water vapor, i.e., *capillary condensation*.[17] This phenomenon is ascribed to the effect of the hydrophobic polymer walls which strongly repulse water molecules, unless the pores are opened upon the sufficient hydration.

Since water penetration into a pore strongly affects its proton conductivity, and the connectivity of the pore network may change with w, one may in principle expect percolation-type phenomena. The experiments show that two categories of material can be distinguished:

Zawodzinski et al.[17] obtain for NAFION and two very similar perfluorinated membranes experimental results which do not show percolation thresholds above water contents of about $w \sim 2-3$. In these samples there is always a finite conductivity except perhaps at very low w. For NAFION the conductivity fit as a function of w is almost a straight line whereas the DOW and the Membrane C-sample possess kinks in this plot which might be an effect of the lower morphological stability due to the lower EW. The conductivity of NAFION at $w \approx 20$ is ~0.07 S/cm. The conductivity of the other two reported membranes is higher in accordance with the smaller EW.

Volfkovich et al.[3] present detailed studies on the structure and transport properties of different samples (heterogeneous MK-40, MA-41, MA-41 I). They found dramatic changes in the swelling behavior with a steep rise of the number of micropores in a small range of increasing w that leads to orders of magnitude increase of the conductivity, thereby clearly displaying the quasi-percolation characteristics of these membranes. The saturation conductivity in the Volfkovich membranes is considerably lower (~ a factor 100) than in the membranes investigated by Zawodzinski.

In principle in any microporous PEM there would be a percolation transition at least due to the total dehydration. However, such a transition would occur at very small overall water contents for which the level of conductivity is far below the required level for the fuel cell performance. From this point of view this region is not so interesting. At high water contents, on the other hand, the percolation effect is practically absent.

Data on geometrical capacity of PEMs are sparse in the literature, since it is hard to distinguish the geometrical capacity of the bulk material from large capacities which are due to thin, poorly hydrated interface layers at the contacts of the membrane to the electrodes. Earlier, Volfkovich et al. presented their capacity data in a form of the membrane dielectric constant, ϵ,[3] which is small at small w ($\epsilon \approx 2-3$) whereas at high w it appeared to be many times larger. Comparing the Volfkovich curves of conductivities and capacities, one finds that a steep rise of capacity usually occurs close to the percolation threshold.

D. Previous Studies. There were a few theoretical studies on percolation effects in PEMs.[18] They presume the existence of a percolation transition and apply the well-known critical laws to the membranes under consideration for the treatment of experimental data.[19] There were no attempts, however, to build a self-consistent theory of conductivity which would relate structural effects and transport mechanisms.

E. The Goal, Approach, and Outline of This Paper. The complex interdependence between w as the external input variable, the morphological structure (EW, pretreatment), and the water structure in the pore−channel network determines the output variable—the overall membrane conductivity, $\sigma(w)$. The directly observable net effect is a strong dependence of the conductivity and related properties on w. Experimental studies demonstrate that this dependence can be completely different for different samples, be it different polymers or only different pretreatment.

Our goal is to establish a consistent framework for the description of the distinct behavior of several membrane-types, which do or do not exhibit percolation phenomena, kinks in the conductivity, etc. A *random network model* could be a suitable approach to this complicated problem. We develop below such a model, which involves main features of the swelling process as well of the proton transport. The key variable is w and the crucial question is, what happens during filling of the microporous structure with water?

There are three main effects of water in PEMs: (i) The *specific properties of water* in the pore−channel system alter with water uptake. (ii) The *pore- and channel-geometries* (diameter, length) change with w. (iii) The *connectivity of the pore−channel network* depends on w. One of the goals of our work is to distinguish the consequences of these different effects establishing the hierarchy of their influence on the membrane conductivity.

We restrict our model to the existence of pores of two "colors": "Red" pores contain only surface hydration water, and they retain their original unswollen shape. "Blue" pores contain in addition bulklike water, and these pores swell for $w > 0$. The different contributions to the conductivities of pores and channels due to the distinction between red and blue pores will be introduced in section II.A. Between the two types of pores we can have three distinct types of bonds, namely, blue−blue, blue−red, and red−red bonds (section II.B). By means of these formal steps the proton transport in the pore−channel network of PEMs is mapped on a site-percolation problem of red and blue sites. The variable which determines the percolation properties of this system is the fraction x of blue pores,

$$x = \frac{\text{number } N_b \text{ of blue pores}}{\text{total number } N \text{ of pores}} \tag{1}$$

Since N_b as well as N depend on w, x is a function of w.

We study the properties of this network in the framework of the pertinent random network theory, section III. The random distribution of bonds is completely determined by the fraction x of blue pores, section III.A. As a first approximation we use the effective medium theory (section III.B) which gives as a result the conductivity of an effective bond.[20] In section III.C we extend the model on the calculation of the imaginary part of admittance. In section IV we discuss model parameters and establish a scheme for their determination. Values for preexponential factors and activation energies of the principal conductivity contributions are extracted from experimental Arrhenius plots (section IV.A) and are used to describe the temperature dependence of the membrane conductivity (section IV.B). Assuming that the conductivities and capacities of the bonds are w-independent, the results are presented as functions of x. Since x is not yet a directly measurable quantity, we must specify how it depends on w for a given membrane. Distinct relationships for this function are suggested in section IV.C on the basis of phenomenological considerations.

By varying the model parameters, we check different options for conductivity, capacity, and full impedance behavior of membranes in section V. Though we primarily focus on NAFION-type membranes, because for these the largest amount of experimental data is available, it is nevertheless important to find out which set of parameter values causes other types of

behavior or which modifications in the theory are required for that. This may give us guidelines for the improvement of membrane performance, some of which are stated in the concluding section.

The properties we actually obtain as results of the effective medium theory are the conductivity and capacity of a single effective bond. These properties are related to the corresponding specific properties of the membrane by sample size and structure-dependent proportionality factors. Unfortunately, these factors will vary with the water content because of swelling. For the fitting of experimental membrane data, we will, therefore, use a simple interpolation scheme: we will fit the theoretical results to the experimental data for the dry and the saturated membrane in order to fix the conductance and capacitance parameters of the model. By this we will automatically retain, for these two limiting cases, the correct proportionality factors between the effective single bond and total membrane properties. At intermediate water contents the elementary conductivities and capacities of network elements mix to give the resulting effective network properties. This procedure already incorporates an interpolation between the two proportionality factors in the dry and in the saturated state. The model systems which are usually considered in the effective medium approximation consist of rigid lattice arrangements, and only the distribution of the distinct elements over the available lattice sites can vary. In the system we consider here, we have to deal with different basic lattice formations plus different distributions of distinct elements over these lattices at different water contents—this complication arising due to swelling.

The goal of the present work is to describe the conductivity dependence on the content of water, homogeneously distributed along the sample, $\sigma(w)$. The results of this study, as well as experimental data on such dependencies,[16,17] can be later used for a parametrization of the dependence of *local* conductivity on *local* water content in representative elementary volumes of the membrane which are large compared to typical pore sizes. Such chracteristics are important ingredients of a phenomenological theory of the proton current through the membrane with account of electroosmosis. Indeed, the conducting protons drag water, which may lead to dehydration of the membrane, predominantly in the layers near the anode. For a given current, a stationary water profile establishes subject to the balance of electroosmotically and pressure (concentration) driven flows. The percolation type dependence of $\sigma(w)$ would thus lead to limiting currents because the water content cannot drop down below the threshold value without blocking the current. Effects of $\sigma(w)$ dependence on the current−voltage characteristics in the presence of electroosmosis have been analyzed in refs 21 and 22 and are also studied in our recent work[23] that investigates the electroosmotic effects in relation to the porous structure of the membrane.

II. The Model

In this section we set the model of conductivity in pores and channels together with the equivalent circuits for the bond conductances, which will be used in the random network description.

A. Conductivities of Network Elements. We start with a discussion of the contributions to conductivity in pores and channels. The absorbed water first wets the inner pore- and channel-surfaces, solvating the SO_3H-groups. A water content $\lambda \approx 5-6$ is needed for this. A stiff "ice-like" water structure forms.[12] We assume that such a sample-spanning surface-water film is established before the membrane actually begins to swell. Then upon further adding of water ($w > 0$) we can distinguish between two types of pores: (i) "red" pores which only contain hydration-water at the surface and (ii) "blue" pores which contain extra-pore water with bulklike properties.

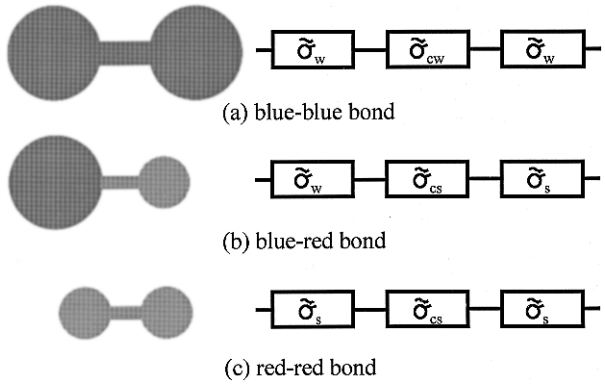

Figure 2. Graphic representations (left) and corresponding equivalent circuits (right) of the three types of bonds between pores.

In red pores and in channels between red pores or between blue and a red pore ("red" channels) the protons are forced to move along the thin surface-water layer, Figure 1. The specific conductivities in these network elements are denoted by σ_s (pores) and σ_{cs} (channels), which may be equal or slightly different, but since the conductivities of the pores and channels depend on their size and shape, we introduce two surface contributions in the network: $\tilde{\sigma}_s$, surface-conductivity of red pores; and $\tilde{\sigma}_{cs}$, surface-conductivity of red channels.

It is imposed that the properties of red network elements do not depend on w. In blue pores and in channels between two blue pores ("blue" channels) the specific conductivities are $\sigma_w(w)$ and $\sigma_{cw}(w)$. Again, different geometry leads to two different conductivities of blue pores and blue channels: $\tilde{\sigma}_w$, conductivity of blue pores; and $\tilde{\sigma}_{cw}$, conductivity of blue channels. We will assume that $\tilde{\sigma}_w(w) > \tilde{\sigma}_s(w)$ and $\tilde{\sigma}_{cw}(w) > \tilde{\sigma}_{cs}(w)$.

B. Connections between Pores, Modeled as Bonds; Bond Conductivities. The random network model of membrane operates with the random distribution of sites, which mimic pores. This determines the distribution of *bonds*, which correspond to connections between pores. Since we are considering only two distinct types of pores, their connections will produce three possible types of bonds which are represented by three elementary equivalent circuits of conductances, shown in Figure 2. The bonds have the following conductivities:

bond between two blue pores

$$\sigma_{bb} = \frac{\tilde{\sigma}_w \tilde{\sigma}_{cw}}{\tilde{\sigma}_w + 2\tilde{\sigma}_{cw}} \tag{2}$$

bond between two red pores

$$\sigma_{rr} = \frac{\tilde{\sigma}_s \tilde{\sigma}_{cs}}{\tilde{\sigma}_s + 2\tilde{\sigma}_{cs}} \tag{3}$$

bond between a blue and a red pore

$$\sigma_{br} = \frac{\tilde{\sigma}_w \tilde{\sigma}_s \tilde{\sigma}_{cs}}{\tilde{\sigma}_w \tilde{\sigma}_s + \tilde{\sigma}_w \tilde{\sigma}_{cs} + \tilde{\sigma}_s \tilde{\sigma}_{cs}} \tag{4}$$

These equations define the single-bond properties. The general relation $\sigma_{rr} \le \sigma_{br} \le \sigma_{bb}$ is obvious.

III. Random Network Theory

A. Distribution of Bonds. We consider the random network of conductances, which are ascribed to the bonds between two

neighboring sites. For the random site distribution, the bond probabilities are expressed through the relative portion of blue pores, x,

$$p_{bb} = x^2 \tag{5}$$

$$p_{rr} = (1 - x)^2 \tag{6}$$

$$p_{br} = 2x(1 - x) \tag{7}$$

The bond probabilities are w-dependent due to the w dependence of x (cf. section IV.C). The distribution function

$$f(\sigma) = p_{bb}(w)\,\delta(\sigma - \sigma_{bb}(w)) + p_{rr}(w)\,\delta(\sigma - \sigma_{rr}(w)) + p_{br}(w)\,\delta(\sigma - \sigma_{br}(w)) \tag{8}$$

defines the probability for a given bond to have a conductivity σ_{bb}, σ_{rr}, or σ_{br}. The task is now to solve the system of Kirchhoff equations for the random network of bond conductances. Generally it can be solved only by computer simulation. In this first paper on the subject, we focus, however, on an approximate analytical solution.

B. Effective Medium Approximation. The simplest approach to deal with the problem is the so-called single-bond effective medium approximation (SB-EMA).[20] In this approximation the Kirchhoff equations are solved for a single bond embedded in an effective medium of the surrounding bonds. The conductivity of an average bond is then determined self-consistently from the condition that fluctuations of the voltage across this bond average out over any region containing many bonds,

$$\int \mathrm{d}\tilde{\sigma}\, f(\tilde{\sigma}) \frac{\sigma - \tilde{\sigma}}{\tilde{\sigma} + (d-1)\sigma} = 0 \tag{9}$$

where $d = z/2$, with z as the number of channels leading to a single pore (in a hypercubic lattice, d denotes the dimension[24]). After the substitution of eq 8 for the distribution function $f(\sigma)$, one obtains an equation on σ:

$$p_{bb}(w)\frac{\sigma - \sigma_{bb}(w)}{\sigma_{bb}(w) + (d-1)\sigma} + p_{rr}(w)\frac{\sigma - \sigma_{rr}(w)}{\sigma_{rr}(w) + (d-1)\sigma} + p_{br}(w)\frac{\sigma - \sigma_{br}(w)}{\sigma_{br}(w) + (d-1)\sigma} = 0 \tag{10}$$

This model gives good results for bond-disordered systems outside the critical region. But it is inaccurate for site-disordered systems that our system belongs to because correlations between the bonds meeting a site are completely neglected. An improvement suggested by Bernasconi and Wiesmann[25] takes into account these types of correlations and is called "low-concentration-cluster" effective medium approximation (LC-EMA). This refined approximation leads, however, to an equation equivalent to eq 10 if one replaces $(d - 1)$ in it by a new dimension-dependent parameter q, which is 1.75 in two dimensions and 3.77 in three dimensions.[26]

A way to test EMA is to see how well it reproduces the exact percolation thresholds, determined numerically, which one obtains in EMA by vanishing two of the three conductivities and calculating the point where $\sigma = 0$. This gives an equation on x, the solution of which is the percolation threshold:

$$x_c = \sqrt{\frac{1}{1+q}} \tag{11}$$

The position of the percolation threshold given by SB-EMA ($q = 2$, $x_c = 0.58$) is considerably larger than the one known from computer simulation. A better (lower) value comes out from LC-EMA ($q = 3.77$, $x_c = 0.46$), but it is still too large.[27] To reproduce the thresholds better, one may treat q as a fitting parameter. For the simple cubic lattice, $x_c = 0.3$, one should take $q = 9.4$. For the fcc lattice, which is a good model for the densely packed structures, $x_c = 0.2$ and $q = 24$. The interpretation of experimental data in the framework of the inverted micellar structure model suggests that the latter case will be the closest approximation to reality.

Equation 10 is cubic in σ. How do we solve it? All conductivities in the linear regime are positively defined, thus the physical solutions for σ must be positive. Furthermore, they are limited by the inequality $\sigma_{rr}(w) \le \sigma(w) \le \sigma_{bb}(w)$. Only one solution of EMA-eq 10 can fulfill these limitations. Indeed, the left side of eq 10 as a function of σ possesses three singularities at negative σ ($q\sigma = -\sigma_{rr}(w)$, $-\sigma_{br}(w)$, $-\sigma_{bb}(w)$). Between two singularities a root of this equation must exist because the value of the function changes from $+\infty$ to $-\infty$ for σ increasing from one singularity to the next. Therefore, two roots are in any case negative and can be excluded as unphysical from the start. To find the remaining root in the general case where the three bond conductivities (eqs 2−4) are nonzero and not equal to each other, one has to use the Cardano formula, which determines, thereby, the explicit $\sigma(w)$ dependence.

Simple analytical expressions may be written in some particular cases. If two bond conductivities are equal or if one bond conductivity is zero, eq 10 reduces to a quadratic equation on σ. The true percolation phenomena occur when the surface conductivities in the red cavities are zero, $\tilde{\sigma}_s$, $\tilde{\sigma}_{cs} = 0$. In this situation the bond conductivities σ_{br} and σ_{rr} are zero and eq 10 reduces to a linear equation, with the solution

$$\sigma(w) = \frac{1}{q}[(1+q)p_{bb}(w) - 1]\sigma_{bb} \tag{12}$$

which has a true percolation threshold given by eq 11. The situation is different for nonzero surface conductivities $\tilde{\sigma}_s$, $\tilde{\sigma}_{cs}$. In this case there is a finite residual conductivity between two red pores, $\sigma_{rr} \neq 0$. This discussion demonstrates already the two main options offered by the introduced model: in the case with vanishing $\tilde{\sigma}_s$, $\tilde{\sigma}_{cs}$ one may expect the *true percolation phenomena*, while for the small but nonzero $\tilde{\sigma}_s$, $\tilde{\sigma}_{cs}$ one may speak only about the *quasi-percolation effect.* If the conductivities of the red cavities ($\tilde{\sigma}_s$, $\tilde{\sigma}_{cs}$) are not small compared to those of the blue cavities ($\tilde{\sigma}_w$, $\tilde{\sigma}_{cw}$), there is no percolation-type variation of conductivity.

C. Frequency Dispersion and Imaginary Admittance. We have considered so far only the DC conductivity. The developed approach, however, can be extended on the calculation of the frequency-dependent complex admittance $y(\omega;w)$ as the solution of eq 10, the real and imaginary part of which give us the conductivity

$$\sigma(\omega;w) = \mathrm{Re}\, y(\omega;w) \tag{13}$$

and the geometrical capacitance

$$C(\omega;w) = \frac{\mathrm{Im}\, y(\omega;w)}{\omega} \tag{14}$$

Within the framework of EMA such an extension is limited to the cases when a DC current can pass through the system (i.e., when the conductivities of the red pores and channels are nonzero or the system is above the percolation threshold), otherwise blocking interfaces will give rise to strong electrical

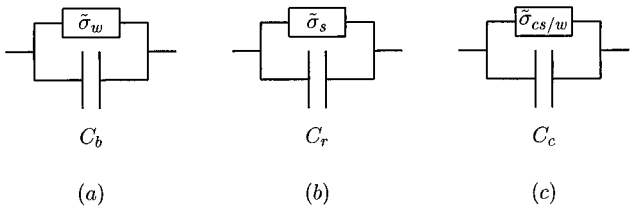

Figure 3. The elements of equivalent circuits with capacitive contributions: (a) blue pore, (b) red pore, (c) channel.

inhomogeneities of the system and the entirely "homogeneous" eq 10 will become misleading.[26,28]

There are different options for the extension of our equivalent circuits. We add capacitances C_b, C_r in parallel to the conductances in the blue and red pores respectively, Figure 3. These capacitances are due to polarizable electrical double layers on the pore surfaces which, however, do not block the current passage through the pores. Another source of capacitance are the hydrophobic PTFE-parts of the membrane which have been considered as inert constituents so far. To take them into account we consider the pores as coated with insulating dielectric layers of polymer material. The coatings are introduced in the equivalent circuits as capacitances C_c in parallel to the channel conductances, Figure 3. None of these new elements gives rise to blocking capacitances in the network as long as the red network elements are conducting.

For the complex admittances of the three bonds, we therefore obtain:

$$y_{bb} = \frac{(\tilde{\sigma}_w + i\omega C_b)(\tilde{\sigma}_{cw} + i\omega C_c)}{(\tilde{\sigma}_w + i\omega C_b) + 2(\tilde{\sigma}_{cw} + i\omega C_c)} \tag{15}$$

$$y_{rr} = \frac{(\tilde{\sigma}_s + i\omega C_r)(\tilde{\sigma}_{cs} + i\omega C_c)}{(\tilde{\sigma}_s + i\omega C_r) + 2(\tilde{\sigma}_{cs} + i\omega C_c)} \tag{16}$$

$$y_{br} = \frac{(\tilde{\sigma}_w + i\omega C_b)(\tilde{\sigma}_s + i\omega C_r)(\tilde{\sigma}_{cs} + i\omega C_c)}{(\tilde{\sigma}_w + i\omega C_b)(\tilde{\sigma}_s + i\omega C_r + \tilde{\sigma}_{cs} + i\omega C_c) + (\tilde{\sigma}_s + i\omega C_r)(\tilde{\sigma}_{cs} + i\omega C_c)} \tag{17}$$

The physical origin of the pore-capacitances C_b and C_r is the double-layer formation at the inner pore surfaces. The flexible dipoles (or "zwitterions") of hydrated fixed ionic groups and mobile hydrated protons form a layer polarizable in an external electric field. As C_b and C_r depend on the density of dipoles (i.e., the number of SO_3^--groups per unit surface area), the thickness δ of the double layer, and the dielectric constant in the double layer, they may in principle be complicated functions of water content. To take into account all these dependencies, we would have to introduce additional parameters. We avoid this, considering only two distinct, *w*-independent capacitances of the pores. For reasons of simplicity we will put $C_r = C_c$ throughout this paper, unless otherwise stated. In red pores the surface water structure is more rigid. The double layer is less polarizable, and the capacitance may be considerably smaller.

The only restriction on the values of the EMA-solution $y(w,\omega)$ comes from the condition Re $y(w,\omega) > 0$ which helps us to single out the only physically correct solution.

IV. Basic Expressions for the Membrane Conductivity

A. Elementary Conductivities: Size Effect, Temperature Depedence, etc. In section II.A we introduced four conductivities, $\tilde{\sigma}_s$, $\tilde{\sigma}_{cs}$, $\tilde{\sigma}_w$, and $\tilde{\sigma}_{cw}$, for the network elements. In the most general case these conductivities can differ due to distinct water structure and different geometries of the water containing cavities (pores and channels).

In principle all four conductivities are due to surface contributions. In blue cavities protons could move in principle through the whole volume. Due to the hydration layers between fixed SO_3^--groups and protons the Coulombic interaction between them is smaller than in the case of bare ions. But the residual Coulombic interaction can still be 1 order of magnitude larger than thermal energies. Therefore, diffusion of protons into the bulk of blue cavities is limited by energy constraints. Hence, true bulk contributions to the conductivity are likely to be small, and we suppose a surface-dominated mechanism. Nevertheless, *the bulk water assists the surface conductivity*: filled blue pores and channels contain more water and therefore provide more degrees of freedom for proton transport. The probability to find degrees of freedom with low activation energies is thus enhanced.

The obvious distinction we have to incorporate exists between σ_s and σ_w. At the moment it is not known how a difference in the structure of pores and channels (density of SO_3^--groups at the surface, geometry, etc.) affects specific properties of water and proton transport mechanisms (preexponential factor, activation energy) in them. Thus, to reduce the number of model parameters, we shall put $\sigma_{cs} = \sigma_s$ and $\sigma_{cw} = \sigma_w$. Moreover, we assume that the *specific* properties (σ_s, σ_w) are *w*-independent.[29]

The properties of red pores and channels are assumed not to change with *w*. Therefore, $\tilde{\sigma}_s$ and $\tilde{\sigma}_{cs}$ are *w*-independent. Different geometries of blue pores and channels lead to different *w* dependencies of the corresponding conductivities of them. If the thickness δ_b of the surface layer to which proton transport is confined is small compared to the radii of pores, the conductivity of the spherical blue pores is independent of their radius r_p

$$\tilde{\sigma}_w \approx 2k_p\delta_b\sigma_w, \quad \delta_b \ll r_p \tag{18}$$

with a constant $k_p \simeq 1$. The conductivity of the channels depends on their radius r_c and length l_c as

$$\tilde{\sigma}_{cw} = \pi\frac{\delta_b(2r_c - \delta_b)}{l_c}\sigma_w \tag{19}$$

which reduces to

$$\tilde{\sigma}_{cw} \approx 2\pi\delta_b(r_c/l_c)\sigma_w, \quad \delta_b \ll r_c \tag{20}$$

in the thin surface limit. If the surface conducting layers are not thin compared to the radii r_p and r_c, then the conductivities would approach the bulklike behavior

$$\tilde{\sigma}_w = k_p'\pi r_p\sigma_w, \quad \delta_b \approx r_p \tag{21}$$

in the pores ($k_p' \simeq 1$) and

$$\tilde{\sigma}_{cw} = \pi(r_c^2/l_c)\sigma_w, \quad \delta_b \approx r_c \tag{22}$$

in the channels.

For an estimate we compare the magnitudes of conductivities in the thin surface limit. Assuming thicknesses $\delta_r = 0.3$ nm and $\delta_b = 0.6$ nm of the double layers in red and blue cavities we obtain $\tilde{\sigma}_s = (0.6\text{ nm})\sigma_s$, $\tilde{\sigma}_{cs} = (0.66\text{ nm})\sigma_s$, $\tilde{\sigma}_w = (1.2\text{ nm})\sigma_w$, and $\tilde{\sigma}_{cw} = (1.13\text{ nm})\sigma_w$ (we put $k_p = 1$, $l_c = 1$ nm, and $r_c = 0.5$ (0.6) nm in red (blue) channels). Thus, we see that conductivities of pores and channels of the same color are of the same order of magnitude ($\tilde{\sigma}_s/\tilde{\sigma}_{cs}$, $\tilde{\sigma}_w/\tilde{\sigma}_{cw} \approx 1$). This justifies a start with $\tilde{\sigma}_{cs} = \tilde{\sigma}_s$ and $\tilde{\sigma}_{cw} = \tilde{\sigma}_w$, i.e., with only two distinct

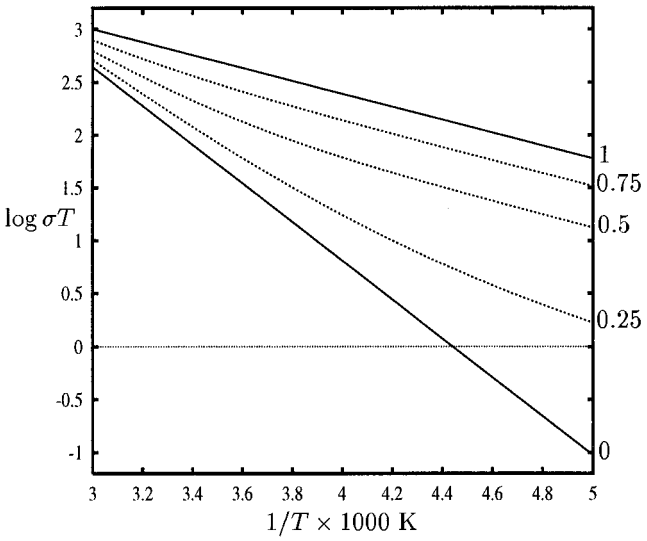

Figure 4. Arrhenius plots of conductivity for different fractions of water-filled pores, x, above the freezing point. Calculated within the effective medium approximation with $q = 24$ in eq 10 and water-content-independent bond conductivities. Conductivity parameters, preexponential factors, and activation energies, fitted to Arrhenius data for NAFION 117, were measured by Cappadonia et al.[16] for a dry membrane ($x = 0$, eq 23) and for a water-saturated membrane ($x = 1$, eq 24).

conductivities, one for the red ($\tilde{\sigma}_s$) and the other one for the blue ($\tilde{\sigma}_w$) pores and channels.[10]

Estimates of preexponential factors[30] and activation energies which determine the temperature dependence of $\tilde{\sigma}_s$ and $\tilde{\sigma}_w$ can be obtained from Arrhenius plots for the membrane-conductivity prior to the solution of the random network model. Indeed, two limiting cases may be taken for orientation. When the membrane is dry except for the surface hydration water ($x = 0$), the membrane conductivity is proportional to $\tilde{\sigma}_s$. On the other hand, the conductivity of the water saturated membrane ($x = 1$) is proportional to $\tilde{\sigma}_w$. The data of Cappadonia et al.[16] for NAFION 117 membranes give us, thereby,

$$\tilde{\sigma}_s T = 4.18 \times 10^8 \, e^{-4222K/T} \Omega^{-1} K \qquad (23)$$

$$\tilde{\sigma}_w T = 2.05 \times 10^5 \, e^{-1407K/T} \Omega^{-1} K \qquad (24)$$

The temperature range where these fits are valid is limited below by the corresponding (w-dependent) freezing temperatures. The upper limit is set by the temperature at which the ion-clustered membrane structure becomes unstable.[31] The main contribution to the w-dependence of the membrane conductivity will come through the dependence of x on w as far as we use the thin surface approximation, eqs 18 and 20. However, we shall consider, for the sake of comparison, also the approximations of eqs 21 and 22, where $\tilde{\sigma}_w$ and $\tilde{\sigma}_{cw}$ depend on w through r_p, r_c, and l_c (cf. section V).

With w-independent bond conductivities we can present the general solution of the EMA-eq 10 in terms of x with the conductivity ratio $\tilde{\sigma}_w/\tilde{\sigma}_s$ as the only free parameter.

B. Discussion of Temperature and x Dependence in EMA. Arrhenius plots for the solution of the EMA-eq 10 are shown in Figure 4 for different values of the ratio $\tilde{\sigma}_w/\tilde{\sigma}_s$ with x as parameter. The lowest curve is the fit of the experimental data for the dry membrane ($x = 0$), eq 23. Upon increasing x the family of curves with increasing conductivities is obtained. In Figure 4 the curve for the water-saturated membrane ($x = 1$) is the fitted curve corresponding to the fit-eq 24. Upon increasing temperature the conductivities increase on all curves, while the

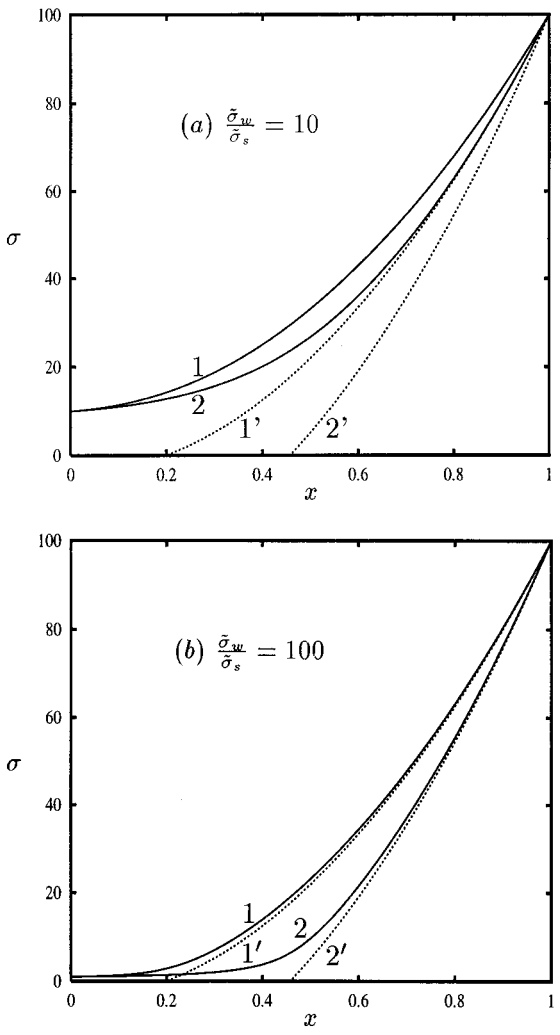

Figure 5. Conductivity dependence on the fraction x of water-filled pores. The solutions of the effective medium approximation, eq 10 with $q = 24$ (densely packed system, curve 1) and $q = 3.77$ (local cluster effective medium approximation, curve 2), are shown in the case of water-content-independent conductivities of the network elements. Conductivity ratio $\tilde{\sigma}_w/\tilde{\sigma}_s$ = (a) 10, (b) 100. Corresponding true percolation cases ($\tilde{\sigma}_s = 0$) are shown for comparison (curves 1′ and 2′).

range of the conductivity variation with x becomes smaller. If we extrapolate the Arrhenius plots to higher temperatures we will reach a temperature where they merge in one point and where no x- and, therefore, no w-dependence is left. The reason for that is simple. With the temperature increase, the difference between the two principal conductivity contributions $\tilde{\sigma}_s$ and $\tilde{\sigma}_w$ becomes smaller, eqs 23 and 24, and, thereby, the dependence on x and w becomes weaker. These plots are in qualitative accordance with experimental findings.[16]

A striking feature of the calculated curves at intermediate x is their curvature, the upturn of the curves with increasing inverse temperature. At intermediate x the system is a mixture of elements with different conductivities according to eqs 23 and 24. Upon decreasing T the contribution of the elements with the lower activation energy (the blue ones) becomes more and more dominant. In our model this upturn tendency could only be avoided by the use of non-Arrhenius-type conductivity parametrizations.

In Figure 5 we show the x dependence of conductivity at different ratios $\tilde{\sigma}_s/\tilde{\sigma}_s$. We compare curves for different values of q, (24, curve 1; 3.77, curve 2), and, therefore, different critical fractions x_c (cf. eq 11 and the corresponding discussion). For

a large ratio between the conductivities the quasi-percolation behavior is evident by comparison with the true percolation cases ($\tilde{\sigma}_s$, $\tilde{\sigma}_{cs} = 0$, no residual conductivity through the red parts of the membrane, corresponding to curves 1′ and 2′).[32] With higher q the critical fraction x_c of blue pores is shifted to smaller values, eq 11.

C. Modeling Swelling Effects. For a comparison with experimental data for membrane conductivity and capacitance as functions of w, we have to specify the relation between the fraction of blue pores, x, and w, $x(w)$. With such a relation at hand we will also be able to study the effects due to w dependence of elementary conductivities ($\tilde{\sigma}_w(w)$, $\tilde{\sigma}_{cw}(w)$) (cf. section V). Besides the question whether the surface conductivity of red cavities is zero or not, the description of the single-bond properties will be the same for different membranes; only values of parameters would vary. Strong differences, however, may be manifested through different effects of swelling on the membranes inner geometry. These would depend on whether the membrane consists of strongly or weakly cross-linked polymer material, whether swelling can be ascribed to the increase and reorganization of already existing pores or whether it is due to the formation of new pores, etc.

The following variables/parameters will be used:

$N(w)$, the total number of pores in the sample (blue and red ones) with N_0 being the total number of pores in the dry membrane ($N(w=0)$).

$Z_{SO_3^-}$, the total number of SO_3^--groups.

$n(w)$, the number of SO_3^--groups per pore; there is experimental evidence that this number grows with w (because the number of pores decreases). This growth is accounted for by a function $g(w) = (n(w)/n_0) - 1$, where $n_0 = n(w=0)$.

$\upsilon(w)$, the pore volume without the hydrated surface volume, i.e., the volume which is filled by extra pore water; $\upsilon_0 = \upsilon(w=0)$ is the residual volume of red pores. The relative pore expansion is accounted for by a function $f(w) = \upsilon(w)/\upsilon_0$.

$x(w)$, the fraction of water-filled pores; $x(w)N(w)$ is the number of blue pores and $(1 - x(w))N(w)$ is the number of red pores.

We make the following assumptions:

(i) The membrane is prepared in such a way that a pore−channel structure exists in the dry state.[8,17] Although the inverted micellar structure might be distorted to a certain degree in the dry state (because this structure is stabilized by the uptaken water), we assume that a system of sample spanning conductive paths remains intact upon drying.

(ii) The majority of SO_3^--groups are located inside pores and channels. We shall adopt the "conservation law" that $Z_{SO_3^-}$ stays constant upon swelling.

(iii) The swelling of pores is only due to extra pore water, $w > 0$.

(iv) All SO_3^--groups throughout the sample are equally hydrated.

(v) In red pores the number n_0 of SO_3^--groups and the radius r_0 (volume υ_0) do not change. Only blue pores swell with w, their growth accounted for by $n(w)$ and $\upsilon(w)$.

The quantities $Z_{SO_3^-}$, $n(w)$, and $\upsilon(w)$ are to be parametrized according to experimental data. One can then find the unknown functions $N(w)$ and $x(w)$ by using two equations. The first one comes out from the conservation of the total number of SO_3^--groups

$$Z_{SO_3^-} = N(w)\, n_0(1 + x(w)\, g(w)) = N_0 n_0 \qquad (25)$$

The second equation results from the proportionality of the total extra water volume in blue pores to w

$$x(w)\, N(w)\, f(w) = N_0 \gamma w \qquad (26)$$

with the proportionality factor

$$\gamma = \frac{m_{\text{dry polymer}}}{N_0 \upsilon_0 \rho_{H_2O}} \qquad (27)$$

The system of these two equations gives

$$N(w) = N_0 \left(1 - \gamma w \frac{g(w)}{f(w)}\right) \qquad (28)$$

and

$$x(w) = \gamma w \frac{\upsilon_0}{\upsilon(w)} \frac{N_0}{N(w)} \qquad (29)$$

$$= \frac{\gamma w}{f(w) - \gamma w g(w)} \qquad (30)$$

In a rigid microporous system in which the morphological structure does not change with water uptake the volume υ and the number of pores N remain constant ($g(w) = 0$, $f(w) = 1$) and thus

$$x(w) = \gamma w \qquad (31)$$

However, in an elastic, weakly cross-linked membrane we have two additional factors (rhs of eq 29) affected by swelling: $\upsilon(w)^{-1}$, $N(w)^{-1}$. Their origin is simple: an increase in the volume of each single-blue pore with w tends to decrease the fraction of blue pores. On the other hand, a decrease of the total number of pores with w will tend to increase $x(w)$. The competition between these two effects will determine the deviation of the $x(w)$ dependence from linearity.

A decrease in the total number of pores upon swelling is due to coalescence of smaller pores into larger pores. How do we know that? This follows from experimental observations which show that the number of SO_3^--groups per one pore increases upon swelling at the constant value of the total number of these groups.[8] Gierke and Hsu[4] calculated average properties of pores from measured Bragg-spacings and macroscopic properties of the membrane (fractional volume change ΔV, fractional weight gain Δm, density of dry polymer, density of water, etc.). They determined values for the average number of SO_3^--groups per pore, $\bar{n}$, and for the average pore radius, $\bar{r}$, at different w, which demonstrate that both properties increase roughly linearly with w. The way, how they obtained these empirical relations implied a model in which the pores sat on average at the sites of a simple cubic lattice with a lattice spacing that was determined by the observed Bragg peaks. No distinction was made between the pores on different sites. This model, therefore, supports the idea of a "homogeneous" membrane in which all pores swell equally. However, the interpretation of experimental data in these terms leads to a controversy. To demonstrate this, we use eqs 25 and 26 which lead to inconsistent equations on the total number of pores as a function of w if we invoke linear relationships for $\bar{n}(w)$ and $\bar{r}(w)$

$$(i)\ \text{eq } 25 \Rightarrow N(w) \propto 1/w$$

$$(ii)\ \text{eq } 26 \Rightarrow N(w) \propto 1/w^2$$

In this paper, we use another model for the description of the membrane structure which avoids this contradiction by considering two distinct species of pores: nonswelling (red) pores and swelling (blue) pores. An argument in favor of this

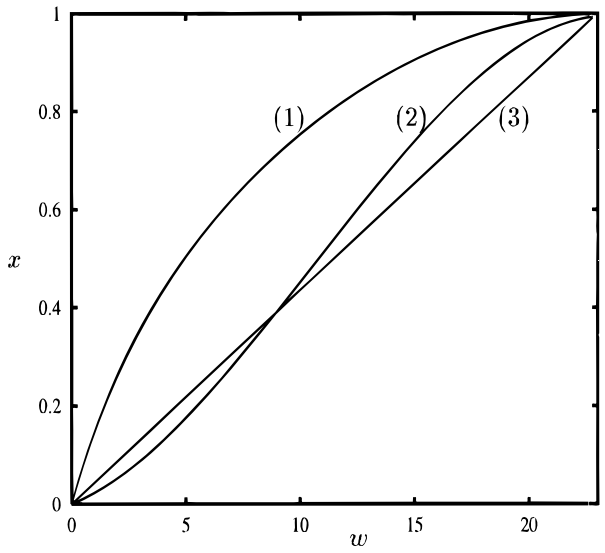

Figure 6. Fraction of water-filled pores, x, as function of water content, w. Curves correspond to the different parametrizations: eq 30 (1), eq 37 (2) with parameters $\alpha = 0.0668$, $\beta = 0.0494$, and $\gamma = 0.167$; (3) depicts the linear dependence in the nonswelling case, $x(w) = (1/23)$-w.

"heterogeneous" model is the tendency to minimize the energetically unfavorable interface between water and hydrophobic PTFE-regions which hinders the extra water from filling all pores equally. The equilibrium size of the water filled pore is determined by the balance between elastic forces exerted by the polymer matrix and "osmotic" pressure inside the pores (formed by the attraction of the hydrophobic polymer walls in water,[12] attractive van der Waals forces, and repulsive hydration forces).[33,34] For a limited amount of water, pores which are smaller than the typical equilibrium size would be unstable. It is thus energetically more favorable to fill a part of the pores with their consequent swelling up to the equilibrium radius than to fill all pores which would have the radius smaller than the equilibrium one.

Equation 29 provides us with the $x(w)$ dependence, if we know the functions $v(w)$ and $N(w)$. To parametrize them we may try to use the data generated by Gierke and Hsu.[4] The w dependencies of these data may be fitted by expressions

$$\bar{n}(w) - n_0 = n_0\,\bar{g}(w) = n_0 \alpha w \tag{32}$$

for the mean increase of the number of SO_3^--groups per pore and

$$\bar{v}(w) = v_0\,\bar{f}(w) = v_0(1 + \beta w)^3 \tag{33}$$

for the mean volume of pores. Let us first identify these properties with the properties of blue pores. Thus, setting $\bar{g}(w) = g(w)$, $\bar{f}(w) = f(w)$ and inserting eqs 32 and 33 in eqs 28 and 30, we obtain the curve shown as (1) in Figure 6, where, to fit the Gierke data, we put $\alpha = 0.0668$, $\beta = 0.0494$, $\gamma = 0.167$. However, taking our model seriously we cannot simply use the mean properties $\bar{n}(w)$, $\bar{v}(w)$ which do not account for the distinction between red and blue pores. It is unclear to which extent the structural properties calculated by Gierke are average properties of all pores or properties of blue pores only (since in our model only these pores are responsible for the swelling). We thus may try to use another parametrization in which blue pores and red pores are assumed to contribute to $\bar{g}(w)$ and $\bar{f}(w)$ with weights x and $(1 - x)$, respectively. With eqs 25 and 26 and the two additional equations

$$v_0\bar{f}(w) = x(v(w) - v_0) \tag{34}$$

$$n_0\bar{g}(w) = x(n(w) - n_0) \tag{35}$$

for the weighting of pore properties of red and blue pores we find the modified relations

$$N(w) = \frac{N_0}{1 + \bar{g}(w)} \tag{36}$$

$$x(w) = \gamma w\{1 + \bar{g}(w)\} - \bar{f}(w) + 1 \tag{37}$$

This $x(w)$ relation is depicted as (2) in Figure 6 (with the same parameters α, β, γ).

The curves depicted in Figure 6 show that different interpretations of experimental data for the morphological structure lead to different $x(w)$ plots. The reference plot for the nonswelling case (eq 31) is shown by (3) (with $\gamma = 1/23$). For the cases depicted in Figure 6, the percolation thresholds in w, as calculated by using eq 11 to obtain x_c and solving then eq 29 for w_c, are (1) $w_c = 1.4$ (for $q = 24$) and 4.3 ($q = 3.77$), (2) 5.5 and 10.1, (3) 4.6 and 10.5. For a particular membrane sample the form of $x(w)$ dependence may not follow any of the derived swelling formulas, eqs 30 and 37, and the best would be to use direct experimental data for this dependence. Without them, it makes sense to classify the result subject to alternative variants of swelling behavior, which is what we essentially did.

V. Results

We first present the results of the calculation of DC conductivity. For this case we show the effect of different types of swelling behavior and of the w dependence of the blue network elements. After that we show the calculated complex admittance at nonzero frequency. Conductance and capacitance parameters in this section will be given in dimensionless units. The conductance parameters can be easily adapted to physical units by taking reasonable values for the conductivity of a saturated membrane sample ($\tilde{\sigma}_w$ has to be taken as three times this value, cf. equivalent circuit for a blue−blue bond in Figure 2) and the residual conductivity of the dry sample ($\tilde{\sigma}_s$ is three times this value, cf. Figure 2), respectively. In the same way the capacitance parameters can be fixed. The alternative approach to fix parameters of the random network elements is to use parameters calculated from microscopic considerations of elementary charge transfer processes and dielectric relaxation processes in the pores together with their geometrical properties.

A. DC Conductivity. Figure 7 depicts the solutions of the EMA-eq 10 for $\sigma(w)$ with w-independent conductivities of all network elements at $\tilde{\sigma}_w/\tilde{\sigma}_s =$ (a) 10 and (b) 100. The curves (1) to (3) correspond to the different $x(w)$ plots shown in Figure 6. In (a) the quasi-percolation type behavior is practically absent, whereas in (b) it is rather obvious with only small deviations from the true percolation case arising close to the percolation threshold.

What will happen if we allow for a w dependence of the conductivities of the blue network elements? Let us attribute such dependencies to $\tilde{\sigma}_w$ and $\tilde{\sigma}_{cw}$ according to phenomenological equations

$$\tilde{\sigma}_w = w^{\nu_p}\sigma_w \tag{38}$$

$$\tilde{\sigma}_{cw} = w^{\nu_c}\sigma_w \tag{39}$$

The exponents ν_p and ν_c account for the w dependence of the geometric properties of blue pores and channels, respectively.

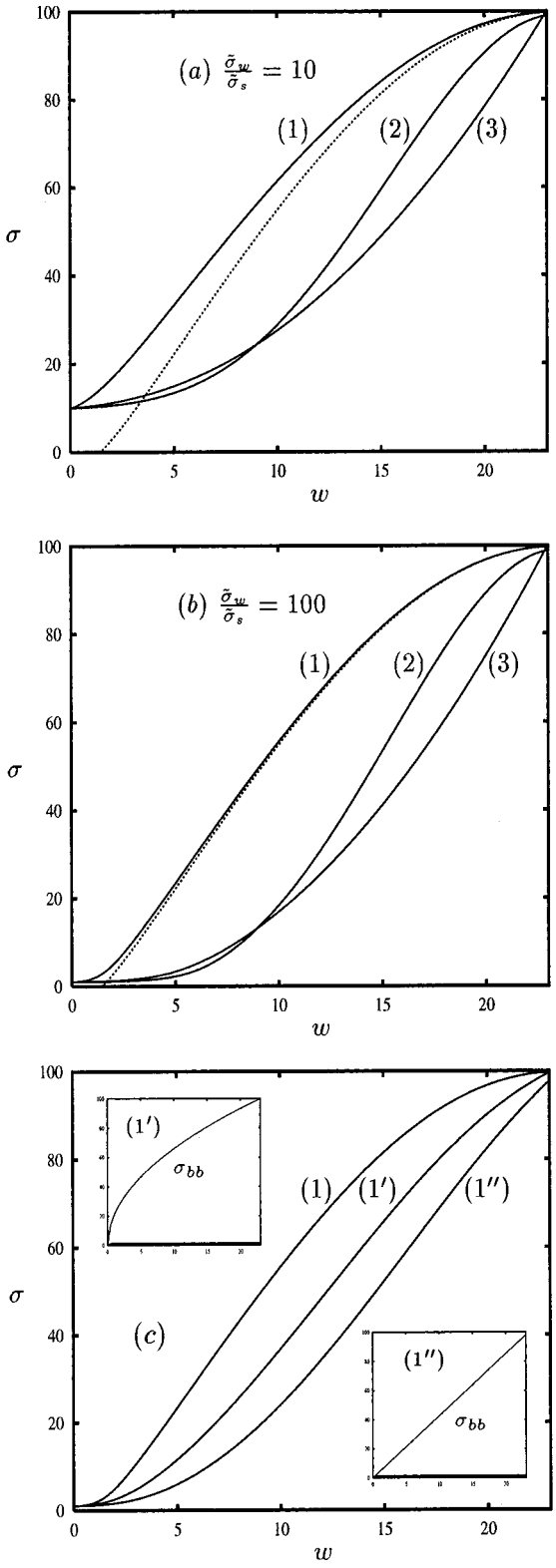

Figure 7. Conductivity as a function of water content, $\sigma(w)$, obtained in effective medium approximation, eq 10, with $q = 24$. (a) and (b) demonstrate the effect of different types of swelling behavior, giving (1) to (3) corresponding to the cases shown in Figure 6. (1) is compared with the true percolation case ($\tilde{\sigma}_s = 0$), dotted line. $\tilde{\sigma}_w/\tilde{\sigma}_s =$ (a) 10, (b) 100 (quasi-percolation effect). (c) shows the consequences of water content dependence of conductivities of the network elements. The reference curve is (1) of (b). The other two curves are obtained with eqs 38 and 39 and (1′) $\nu_p = \nu_c = 0.5$ ($\sigma_w = 62.5$), (1″) $\nu_p = \nu_c = 1$ ($\sigma_w = 12.8$). The parameter σ_w is fitted to merge all four curves in the saturation region (at $w = 23$).

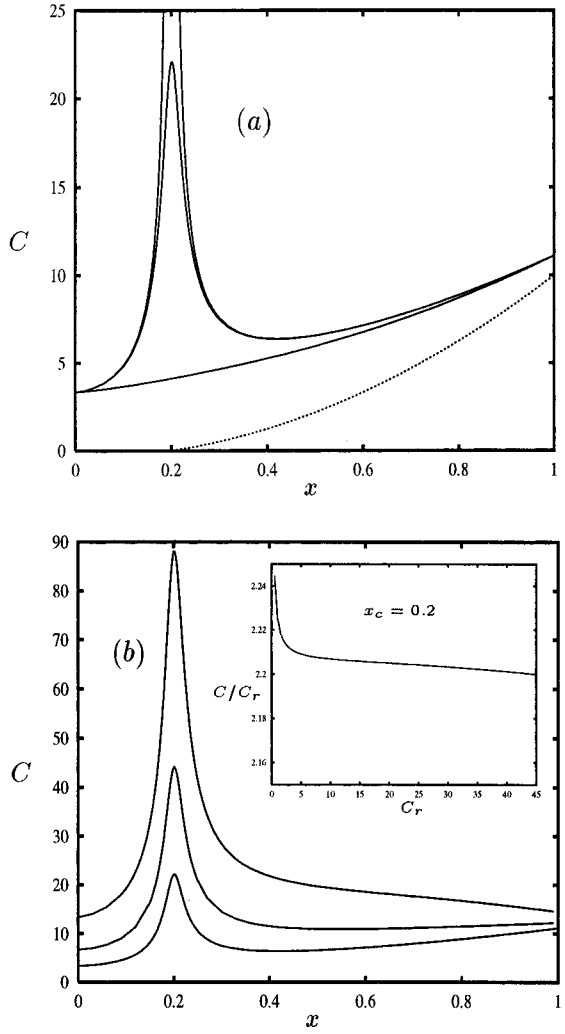

Figure 8. Geometrical capacity as a function of the portion of water filled pores, x, calculated in effective medium approximation, eq 10 ($q = 24$). (a) Conductivity parameters are the same as in Figure 5, $\tilde{\sigma}_w/\tilde{\sigma}_s = 10$ (solid curve without maximum), 3000 (solid curve with maximum). The capacities of the network elements, are $C_b = 45$, $C_r = C_c = 10$ for these curves. With $\tilde{\sigma}_s = 0$, the maximum at the percolation threshold develops into a "singularity", but the effective medium approximation breaks down in this case. If in addition $C_r = C_c = 0$, the maximum vanishes (dotted line with percolation dependence). (b) The effect of C_r on the heights of the maximum for $\tilde{\sigma}_w/\tilde{\sigma}_s = 3000$, $C_b = 45$ and $C_r = C_c = 10$, 20, 40. The dependence of the proportionality factor between maximum height and C_r on C_r is depicted as an inset.

They regulate the interplay between the surface and bulk conductivity mechanisms (cf. section IV.A). For the illustration of effects of w dependence of bond conductivities we put (1) $\nu_p = \nu_c = 0$ ($\sigma_w = 300$, the previous case of Figure 7b), (1′) $\nu_p = \nu_c = 0.5$ ($\sigma_w = 62.5$, to obtain the same saturation value of conductivity), (1″) $\nu_p = \nu_c = 1.0$ ($\sigma_w = 12.85$).[10]

B. AC Admittance. The capacity C, eq 14 in the zero-frequency limit (far below all characteristic frequencies of the system), shows two remarkable features: an overall increase with w, the magnitude of which depends on the ratio C_b/C_r ($C_r = C_c$) between the capacitance parameters, and in certain cases a sharp maximum at the percolation threshold the height of which depends on the relation between the ratios $\bar{\sigma}_s/C_r$ and $\tilde{\sigma}_w/C_b$. The smaller the first ratio is compared to the latter, the higher the maximum.

In Figure 8, C is shown as a function of x. The capacitance parameters due to red pores and channels are taken to be $C_b = 45$ and $C_r = C_c = 10$ in dimensionless units. $C(x)$ grows monotonously with x (and w) if the ratio $\tilde{\sigma}_w/\tilde{\sigma}_s$ is not too large

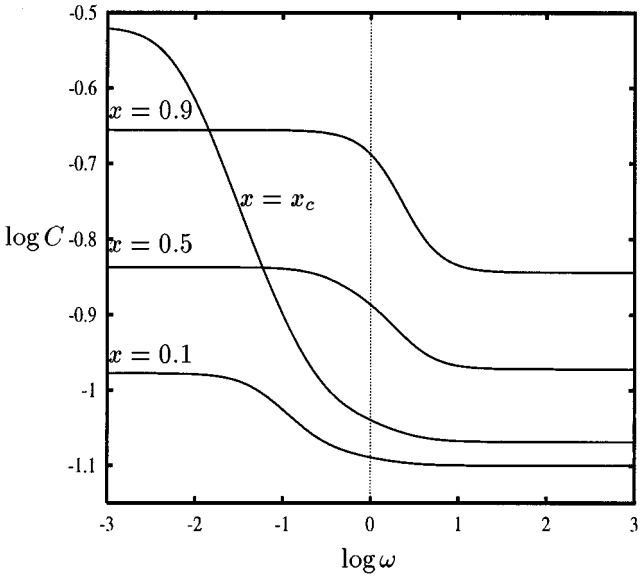

Figure 9. Double-logarithmic plot of the frequency dependence of the capacity at the fractions $x = 0.9, 0.5, 0.2(=x_c), 0.1$. The conductivities of the network elements are $\tilde{\sigma}_w = 1$, $\tilde{\sigma}_s = 0.001$, and capacities are $C_b = 1$, $C_r = C_c = 0.22$.

(10 for curve 1). However, the maximum at the percolation threshold appears for larger $\tilde{\sigma}_w/\tilde{\sigma}_s$ (3000 in Figure 8), which tends to develop into a singularity with $\tilde{\sigma}_w/\tilde{\sigma}_s \rightarrow \infty$ as depicted in Figure 8. The corresponding water content dependencies can be obtained by rescaling the x-axis with the appropriate $x(w)$ dependence. Modification of the swelling behavior, i.e., $x(w)$ dependence (and q), has the same effect as already discussed in the previous section. Indeed, for the swelling pattern given by curve 1 of Figure 6 and for a large value of q the maximum is found for small w, whereas for curve 2 and small q it is at quite high w, see Figure 11 and discussion in section VII.

The maximum (or singularity) at the percolation threshold is only found if the ratio $\tilde{\sigma}_w/\tilde{\sigma}_s$ is large and if the capacitances in channels and red pores are nonzero. With these prerequisites, however, the effective medium approach might become improper below the percolation threshold due to the existence of blocking interfaces (see section III.C). It has to be checked by other methods (e.g., by computer simulation[28]), which would take the inhomogeneities due to blocking elements into account, whether the maximum is not an artifact of the EMA.

Nevertheless, the nature of this striking feature can be rationalized. Right at the percolation threshold there is yet no path through the system which runs exclusively through the well-conducting, less dissipative (i.e., $\tilde{\sigma}_w/C_b$ large) blue network elements. Every possible path through the network of capacitances and conductances is interrupted by at least one highly dissipative red element (where the dissipation is the higher, the smaller $\tilde{\sigma}_s/C_r$). All these interrupting elements are in parallel and they, thus, give rise to a huge effective capacity of the total system. Especially in the case of $\tilde{\sigma}_s = 0$, i.e., when the red elements are pure capacitances, they form an effective capacitance with an infinite surface area which disconnects the sides of membrane and, therefore causes the occurrence of the singularity in capacity at the percolation threshold. This explanation suggests that the capacity at the maximum is roughly proportional to C_r. This is what we actually see in Figure 8b. The proportionality is not fulfilled rigorously, but to a high degree of accuracy (see the inset).

The frequency dependence of the capacity is shown at different x in Figure 9 with the capacitance parameters as in Figure 8 and $\tilde{\sigma}_w/\tilde{\sigma}_s = 1000$. With decreasing x the capacity at a given ω becomes smaller and the critical frequency ω_c which marks the transition from the low-ω plateau to the high-ω plateau decreases. At x_c, the abnormally high zero-frequency value of capacity is found.

The value of ω_c can be estimated if the conductivity and capacity parameters are calculated from microscopic pore properties. From an estimate with $\sigma_w = 0.3$ S/cm, $\delta_b = 5$ Å, $k_p = 2$ in eq 18 for the conductivity and $\epsilon_0 = 8.8542 \times 10^{-12}$ *As/Vm*, $\epsilon_b = 15$, $A_b = 2.5 \times 10^3$ Å^2 for the pore properties which determine the capacitity, $C_b = \epsilon_0\, \epsilon_b(A_b/\delta_b)$, the characteristic frequency due to blue-pore contributions is found to be $\sim 10^9$ s^{-1}.[35]

We present in Figure 10 the Cole−Cole plots corresponding to the curves of Figure 9. At the large fraction $x = 0.9$ in (a) blue−blue bonds dominate the network properties. In principle, contributions due to blue channels and blue pores could be distinguished. If their corresponding relaxation frequencies, $\omega_p = \tilde{\sigma}_w/C_b$ (blue pores) and $\omega_c = \tilde{\sigma}_w/C_c$ (blue channels), are well separated ($\omega_b/\omega_c = 45$ in Figure 10a), two distinct semicircles are resolved (dotted line). However, if ω_b/ω_c is less than ~10,

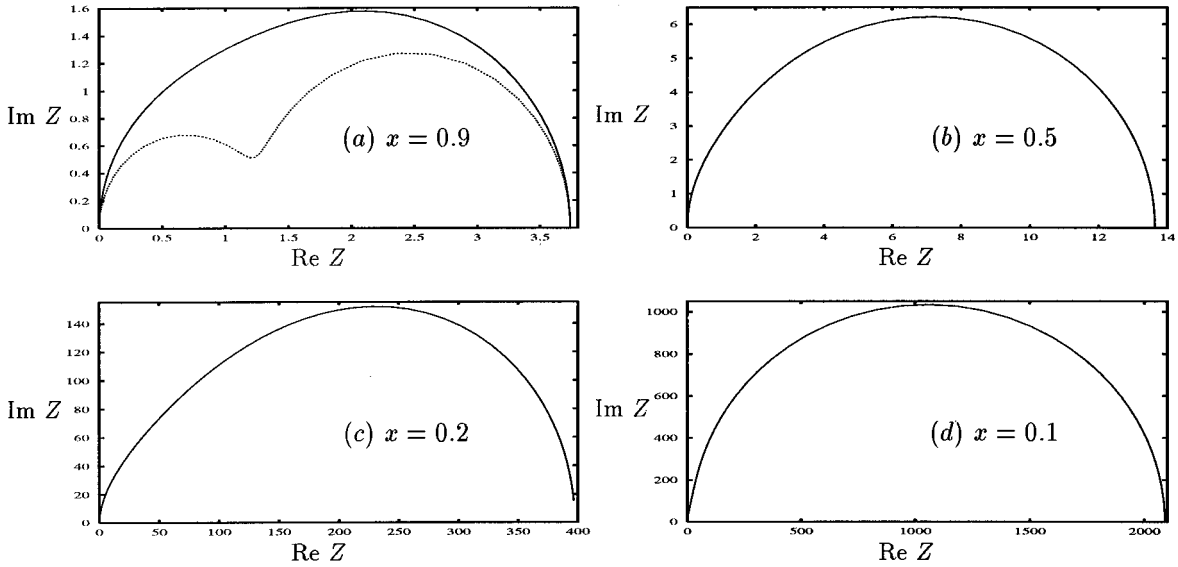

Figure 10. Cole−Cole plots corresponding to the four curves in Figure 9. In (a) the dotted curve with two well-resolved semicircles is obtained with a large ratio of the relaxation frequencies of blue pores and channels (we put this ratio $\omega_b/\omega_c = 45$ here). Solid curves are obtained with the parameters as used in Figure 9.

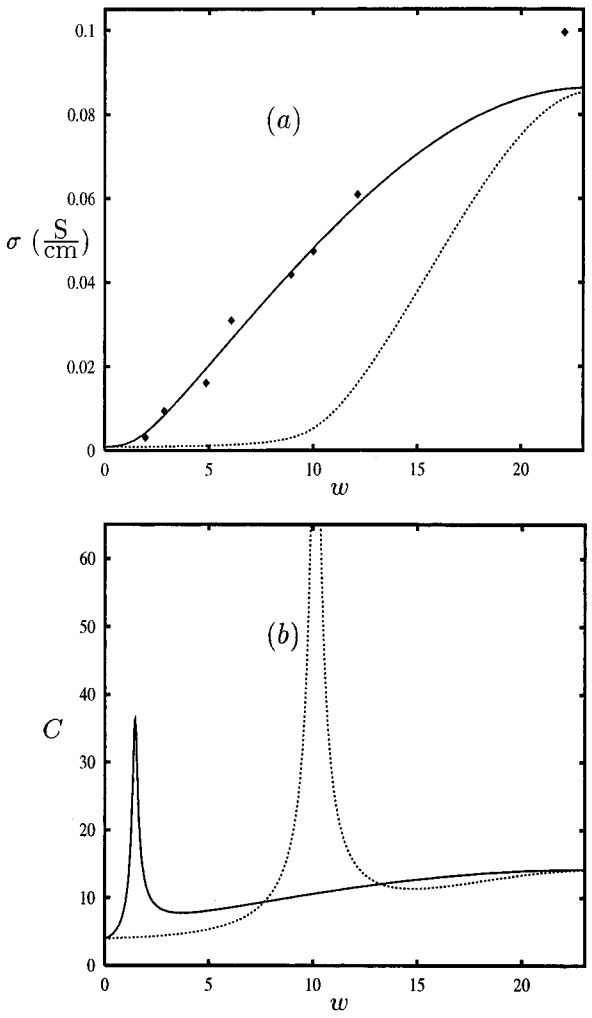

Figure 11. Comparison of different types of behavior of the solution of the effective medium approximation, eq 10, for (a) conductivity and (b) capacity as functions of the water content, with $\tilde{\sigma}_w = 0.26$ S/cm, $\tilde{\sigma}_w/\tilde{\sigma}_s = 6000$ and $C_b = 58$, $C_c = C_r = 12$. The two curves represent two cases: Solid curves correspond to the swelling behavior prescribed by (1) of Figure 6 and good connectivity $q = 24$ (the case of an "elastic" membrane). Dotted curves follow the swelling behavior of (2) of Figure 6 and poor connectivity $q = 3.77$ (the case of a "soft" membrane). The points in (a) are the conductivity data of Zawodzinski for NAFION 117. For the parameter values adopted, the theoretical curve for the behavior of an elastic membrane fits these data.

the semicircles merge, and the distinct contributions cannot be resolved (solid line).

VI. Discussion and Comparison with Experiment

In Figure 11a a fit of the proposed model to the conductivity data of NAFION of Zawodzinski et al.[17] is presented. What information about the membrane properties can we extract from this fit? To obtain a small "critical" water content we used the value $q = 24$ and the swelling parametrization depicted as (1) in Figure 6. The large q value is realized for a tightly packed structure of pores with a high coordination number, thereby providing a good connectivity of the network; the parametrization of swelling is that of an elastic membrane in which water distributes quite homogeneously, providing high values of x already at small w. The saturation value of the conductivity at $w \approx 20$ was obtained with $\tilde{\sigma}_w = 0.26$ S/cm. The conductivity ratio was set to $\tilde{\sigma}_w/\tilde{\sigma}_s = 100$ in order to find the quasi-percolation type behavior at small w.

The other two samples, investigated by Zawodzinski et al.,[17] show kinks in $\sigma(w)$. These samples have a lower EW, which provides higher conductivity but a less stable morphology. Here, the number of SO_3^--groups and the total available pore space are larger. If the conductivity mechanisms are considered to be the same as in NAFION, then the origin of the observed kinks can only be ascribed to effects in swelling behavior.

The membranes studied by Volfkovich[3] have a higher critical water content and show a steep rise of conductivity at intermediate w. The swelling-properties of these membranes appear to be worse. It seems reasonable that the $x(w)$ dependence, as it is depicted as (2) in Figure 6, where the fraction of blue pores increases only slowly at small w, goes together with a small value of the phenomenological parameter q of the EMA, reflecting a poor connectivity of the random network and a small coordination number of sites therein (loose packing of pores which opposes an easy spreading of water in the membrane). This case will be characteristic of "poor wetting". The opposite case, given by curve (1) of Figure 6 for $x(w)$ and $q = 24$ (dense packing of pores, good connectivity), corresponds to "good wetting".

In order to demonstrate the significance of these morphological properties, $x(w)$ and q, the two cases are compared in Figure 11 for conductivity and for capacity. A high percolation threshold in w is obtained with a small q value ($q = 3.77$), and a $x(w)$ dependence depicted as (2) in Figure 6. A small residual membrane conductivity below the percolation threshold is obtained at a large ratio $\tilde{\sigma}_w/\tilde{\sigma}_s$. This case, shown as the dotted line in Figure 11a, would give a steep rise of conductivity by several orders of magnitude at the percolation threshold, but the w dependence well below and above the percolation threshold is weak, which is in line with experimental findings.

We do not have experimental data for the membrane bulk geometrical capacitance to compare with the predictions of our effective medium theory. To extract the geometrical capacitance of the membrane from impedance data, one must go to very high frequencies, in the GHz range. Recently a coaxial probe method was suggested for the impedance spectroscopy in the range of frequencies up to 0.3 GHz.[36] It, thus, may appear to be possible to check the prediction of the anomalous peak of the capacitance, close to the percolation threshold, if the experiments similar to ref 36 will be performed with the variation of the water content.

VII. Conclusions

We have studied a microporous polymer electrolyte membrane as a random network of three elementary types of bonds, representing the conductances between water-filled ("blue") and dry ("red") pores. Specific properties of water in the proton conducting pores and channels as well as the geometrical properties of these network elements were treated on a rather crude level. The remaining parameters which represent these properties in the model are the conductivity $\tilde{\sigma}_w$ of the blue elements of the network and the ratio of conductivities of blue and red pores. We have shown, that connectivity and wetting properties can explain most of experimental observations, in particular, the drastically different behavior of different samples (good vs poor wetting). If we accept the scenario of the network properties, the refinement of the description of wetting and swelling should then be the next step in our work.

An alternative to our model with the two distinct types of pores would be a homogeneous scenario, in which all pores are equal at any water content. Then the network properties would be rather tedious ($x = 1$ at all $w > 0$) but, instead, the single pore and channel properties (specific properties of water therein, which determine mechanisms of proton transport, and geometrical properties) would be the key factors determining

membrane performance. Besides the fact that the homogeneous scenario is energetically unfavorable, it is also questionable, whether it would be able to explain experimental facts.

There are few sources of correlations and fluctuations which we did not discuss in this paper. What is not considered? We have solved the Kirkpatrick problem for a given pore−channel network which is filled with water, but we have not elaborated the problem how this structure is created by the distribution of water in it. Water is delivered from two sides of the thin sheet of membrane. It might, therefore, be an oversimplification to distribute blue pores completely at random in the network. The phenomena of this kind are known to give rise to capillary hysteresis, and they can hardly be ignored when the hysteresis is not small.[37]

By fixing the value of q in the Kirckpatrick equation we specified a lattice type with a certain density of pores. However, upon swelling the pores become more tightly packed and the connectivity will increase on average−although this effect might be partly compensated for with the decrease in the total number of pores. All in all, q may also be water content dependent which will shift the (*quasi*-)percolation threshold. Few other facts which can cause fluctuations were not taken into account: we considered only two distinct types of pores−in reality a complex pore distribution exists; moreover, the effective medium theory neglects fluctuations systematically. Despite these obvious limitations, we think that the model may serve as a starting point for the analysis of electrophysical properties of PEMs in dependence of water content.

What information about the optimal membrane performance can we extract from our results up to this point? In order to reach a high membrane conductivity, $\tilde{\sigma}_w$ should be large. The ratio $\tilde{\sigma}_w/\tilde{\sigma}_s$ (>1) should not be large ($\sim O(1)$) in order to have a small w dependence of the membrane conductivity. This ratio is determined by the different proton transport mechanisms at different w in pores and channels and by the temperature. At higher temperatures (but still in the range of polymer stability), $\tilde{\sigma}_s$ approaches $\tilde{\sigma}_w$. Under such conditions, the water management, i.e., prohibiting "drying out" of the membrane, would not be so critical for the membrane performance. At lower temperatures, small local fluctuations of w, induced by electroosmotic effects, may give rise to drastic changes in the membrane performance.

If $\tilde{\sigma}_w/\tilde{\sigma}_s \gg 1$, the swelling properties of the membrane, represented by $x(w)$ and q, become of primary importance. We will find here a quasi-percolation effect. The percolation threshold, however, can be shoved to very small water contents ($w_c \sim 1$) if there is a good *connectivity of the network* (large q, high coordination of pores) and if the fraction x is large already at small w so that paths of filled blue pores and channels can easily develop. Under such good wetting conditions, no drastic changes in membrane conductivity with decreasing w will appear down to very small w and this still provides good conditions for water management.

The worst case would be a large $\tilde{\sigma}_w/\tilde{\sigma}_s$ ratio combined with bad wetting conditions (small q, small fraction x at small w) which gives a rather sharp percolation threshold at relatively high w with a steep (exponential) increase of σ above w_c. If even the saturation value of conductivity of such a membrane is excellent, the problems of water management in the course of electroosmotic drag and water diffusion would probably make the membrane less attractive for the use in fuel cells.

Returning back to Figure 6, we can make some concluding remarks on microscopic membrane properties which might be responsible for different $x(w)$ dependencies and, therefore, different effects in conductivity and capacitance. The swelling properties of a membrane are determined by the competition between the elasticity of the polymer matrix and the internal "osmotic" pressure in water-filled pores due to hydrophobicity of the polymer material. For a rather elastic polymer material single pores have a smaller equilibrium radius at a given w compared to a softer membrane type. Therefore, the uptaken water fills a larger fraction x of pores, giving large values of x and a good connectivity of the network already at small w. In a soft membrane, on the other hand, the equilibrium radius of pores is larger, and a smaller fraction x of these pores is necessary to take up the water. This leads to inhomogeneous swelling, poorer connectivity of the network, and consequently, poorer performance. Obviously, the proper balance of the factors governing swelling is a very important point in optimization of membrane design.

Acknowledgment. Special thanks to Marcella Cappadonia for helpful advice and consultations. Useful discussions with Semion Gluzman, Alexander Kuznetsov, Vladimir Mazin and Yuri Volfkovich are appreciated. The Research Center "Jülich", Germany, assisted in meeting the publication costs of this article.

References and Notes

(1) Leo, J. M. J.; Mugerwa, M. N.; *Fuel Cell Systems*; Plenum Publishing Corporation: New York, 1993. Schmidt, V. M.; Bröckerhoff, P.; Höhlein, B.; Menzer, R.; Stimming, U. Utilization of Methanol for Polymer Electrolyte Fuel Cells in Mobile Systems. *J. Power Sources* **1994**, *49*, 299. Schmidt, V. M.; Stimming, U. Fuel Cell Systems for Vehicle Applications. In *New promising Electrochemical Systems for Rechargeable Batteries*; Barsukov, V., Beck, F. Eds.; 1996; p 233.

(2) The swelling degree of a PEM depends on the working conditions, the pretreatment, the mechanism of water uptake, etc.

(3) Vol'fkovich, Yu. M. *Elektrokhimiya* **1984**, *20*, 656. Vol'fkovich, Yu. M.; Khozyainova, N. S.; Elkin, V. V.; Berezina, N. P.; Ivina, O. P.; Mazin, V. M. *Elektrokhimiya* **1988**, *24*, 344. Vol'fkovich, Yu. M.; Dreiman, N. A.; Belyaeva, O. N.; Blinov, I. O. *Elelktrokhimiya* **1988**, *24*, 352.

(4) Eisenberg, A., Yeager, H. L. Eds.; *Perfluorinated Ionomer Membranes*; ACS Symposium Series 180; American Chemical Society: Washington, DC, 1982.

(5) Steck, A. E. Membrane Materials in Fuel Cells. In *New Materials for Fuel Cell Systems 1*; Savadogo, O., Roberge, P. P., Veziroglu, T. N., Eds.; Montreal, Quebec, Canada, Editions de L'Ecole Polytechnique de Montreal, 1995; p 74. Kordesch, K.; Simader, G. *Fuel Cells and their Applications*; VCH: Weinheim, 1996; p 72.

(6) Starkweather, H. W., Jr. *Macromolecules* **1982**, *15*, 320.

(7) Pourcelly, G.; Gavach, C. In *Proton Conductors*; Colomban, Ph., Ed.; Cambridge University Press: Cambridge, U.K., 1992, p 294.

(8) Gierke, T. D.; Munn, G. E.; Wilson, F. C. *J. Polym. Sci. Polym. Phys. Ed.* **1981**, *19*, 1687.

(9) Falk, M. *Can. J. Chem.* **1980**, *58*, 1495.

(10) There has never been any direct experimental evidence for the existence of small channels. In this respect any distinction which we would make between pores and channels would be somehow artificial.

(11) Dreyfus, B.; Gebel, G.; Aldebert, P.; Pineri, M.; Escoubes, M.; Thomas, M. *J. Phys. (France)* **1990**, *51*, 1341.

(12) Gompper, G.; Hauser, M.; Kornyshev, A. A. *J. Chem. Phys.* **1994**, *101* (4), 3378.

(13) Kreuer, K. D.; Dippel, Th. Meyer, W.; Maier, J. *Mater. Res. Soc. Symp. Proc.* **1993**, *293*, 273. Kreuer, K. D.; Dippel, Th. Meyer, W.; Maier, J. *ECS Meeting in Chicago*, October 1995. Dippel, Th.; Hainovsky, N.; Kreuer, K. D.; Münch, W.; Maier, J. *Ferroelectrics* **1995**, *167*, 59. Kreuer, K. D.; Proton Conductors−Materials and Applications. *Chem. Mater.* **1996**, *8* (3), 610.

(14) It was suggested that at intermediate−but not too small−water contents the protonic conductivity is highly correlated with molecular diffusion (vehicle mechanism). With increasing water content the contribution of structural diffusion increases.[13]

(15) The proportionality factor is determined by the equivalent weight, $W \sim \mathrm{EW}^{-1}\lambda$. For NAFION with EW 1200, the relation is, for example, $\lambda = {}^2/_3 W$.

(16) Cappadonia, M.; Erning, J. W.; Stimming, U. *J. Electroanal. Chem.* **1994**, *376*, 189. Cappadonia, M.; Erning, J. W.; Saberi Niake, S. M.; Stimming, U. *Solid State Ionics* **1995**, *77*, 65.

(17) Zawodzinski, T. A. Jr.; Springer, T. E.; Uribe, F.; Gottesfeld, Sh. *Solid State Ionics* **1993**, *60*, 199.

(18) Hsu, W. Y.; Barkley, J. R.; Meakin, P. *Macromolecules* **1980**, *13*, 198. Wódzki, R.; Narebska, A.; Kwaś, W. *J. Appl. Polym. Sci.* **1985**, *30*,

769. Gavach, C.; Pamboutzoglou, G.; Nedyalkov, M.; Pourcelly, G. *J. Membrane Sci.* **1989**, *45*, 37.

(19) Stauffer, D.; Aharony, A. *Introduction to Percolation Theory*, revised 2nd ed.; Taylor and Francis: London, 1994.

(20) Kirkpatrick, S.; Percolation and Conduction. *Rev. Mod. Phys.* **1973**, *45* (4), 574.

(21) Verbrugge, M. W.; Hill, R. *J. Electrochem. Soc.* **1990**, *137*, 3770. Bernardi, D. M.; Verbrugge, M. W. In *Proceedings of the Symposium on Modeling of Batteries and Fuel Cells*; White, R. E., Verbrugge, M. W., Stockel, J. F., Eds.; The Electrochem. Soc., Proc. 91-10; 1991; p 240.

(22) Springer, T. E.; Zawodzinski, T. A.; Gottesfeld, S. In *Proceedings of the Symposium on Modeling of Batteries and Fuel Cells*; White, R. E., Verbrugge, M. W., Stockel, J. F., Eds.; The Electrochem. Soc., Proc. 91-10; 1991; p 209.

(23) Eikerling, M.; Kharkats, Yu.; Kornyshev, A. A.; Volfkovich, Yu. M. *J. Electrochem. Soc.*, submitted for publication.

(24) We deal exclusively with 3-dimensional systems.

(25) Bernasconi, J.; Wiesmann, H. J. *Phys. Rev. B* **1976**, *13*, 1131.

(26) Gluzman, S.; Kornyshev, A. A.; Neimark, A. V. *Phys. Rev. B* **1995**, *52* (2), 927.

(27) This value is close to the percolation threshold for site-percolation on a diamond-lattice, $x_c = 0.43$ (coordination number 4).

(28) Abel, J.; Kornyshev, A. A. *Phys. Rev. B* **1996**, *54*, 6276.

(29) Actually, this point is not so critical as it might seem because we can partly retain these dependencies if we introduce *w*-dependencies in $\tilde{\sigma}_w$ and $\tilde{\sigma}_{cw}$ for geometrical reasons, eqs 38 and 39.

(30) These are preexponential factors which were determined for the conductivity of the total membrane. By using them for the parametrizations of the conductivities of the network elements, we have implicitly scaled up the EMA solution to the total membrane size.

(31) Rieke, P. C.; Vanderborgh, N. E. *J. Membrane Sci.* **1987**, *32*, 313.

(32) The critical behavior $\sigma(x) \sim (x - x_c)$ with a critical exponent 1 is a typical result of the effective medium approach. This reflects the deficiency of EMA, since the true conductivity exponent is known to be roughly 2.[19]

(33) Hsu, W. Y.; Gierke, T. D. *Macromolecules* **1982**, *15*, 101.

(34) Rand, R. P.; Parsegian, V. A. *Biochem. Biophys. Acta* **1990**, *988*, 351. Kornyshev, A. A.; Leikin, S. *Phys. Rev. A* **1989**, *40*, 6431. Kornyshev, A. A.; Leikin, S. In *Springer Proc. Phys. 66, Structure and conformation of amphiphilic membranes*; Lipowski, R., Ed.; Springer: Berlin, 1992; p 83. Leikin, S.; Parsegian, V. A.; Rau, D. C.; Rand, R. P. *Ann. Rev. Phys. Chem.* **1993**, *44*, 369.

(35) At low water contents the characteristic frequencies which are due to red pore properties will dominate the overall membrane behavior. Since the conductivity is considerably smaller for these pores, the characteristic frequencies might also be smaller by a few orders of magnitude in this case. But still we can assume that they are too large to be reached by experiment.

(36) Anantaraman, A. V.; Gardner, C. L. *J. Electroanal. Chem.* **1996**, *414*, 115.

(37) Sahimi, M. *Flow and Transport in Porous Media and Fractured Rock*; VCH: Weinheim, **1995**; Chapter 5, 12. Mason, G. *Proc. R. Soc. London A* **1988**, *415*, 453.